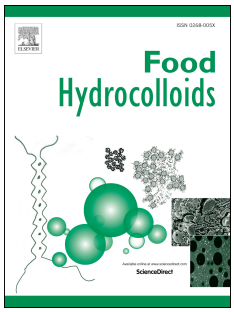

Molecular simulation of partially denatured β-lactoglobulin

Zhuo Zhang, Valeria Arrighi, Lydia Campbell, Julien Lonchamp, Stephen R. Euston

PII: S0268-005X(23)00357-0

DOI: https://doi.org/10.1016/j.foodhyd.2023.108811

Reference: FOOHYD 108811

To appear in: *Food Hydrocolloids*

Received Date: 19 November 2022

Revised Date: 20 April 2023

Accepted Date: 22 April 2023

Please cite this article as: Zhang, Z., Arrighi, V., Campbell, L., Lonchamp, J., Euston, S.R., Molecular simulation of partially denatured β-lactoglobulin, *Food Hydrocolloids* (2023), doi: https://doi.org/10.1016/j.foodhyd.2023.108811.

Author Statements

Zhuo Zhang: Conceptualization; Data curation; Formal analysis; Investigation; Methodology; Roles/Writing - original draft; Writing - review & editing.

Valeria Arrighi: Conceptualization; Funding acquisition; Supervision; Validation; Roles/Writing - original draft; Writing - review & editing.

Lydia Campbell: Conceptualization; Funding acquisition; Methodology; Supervision; Validation; Roles/Writing - original draft; Writing - review & editing.

Julien Lonchamp: Conceptualization; Supervision; Roles/Writing - original draft; Writing - review & editing.

Stephen R. Euston: Conceptualization; Data curation; Formal analysis; Funding acquisition; Methodology; Project administration; Resources; Supervision; Validation; Visualization; Roles/Writing - original draft; Writing - review & editing.

Graphical Abstract

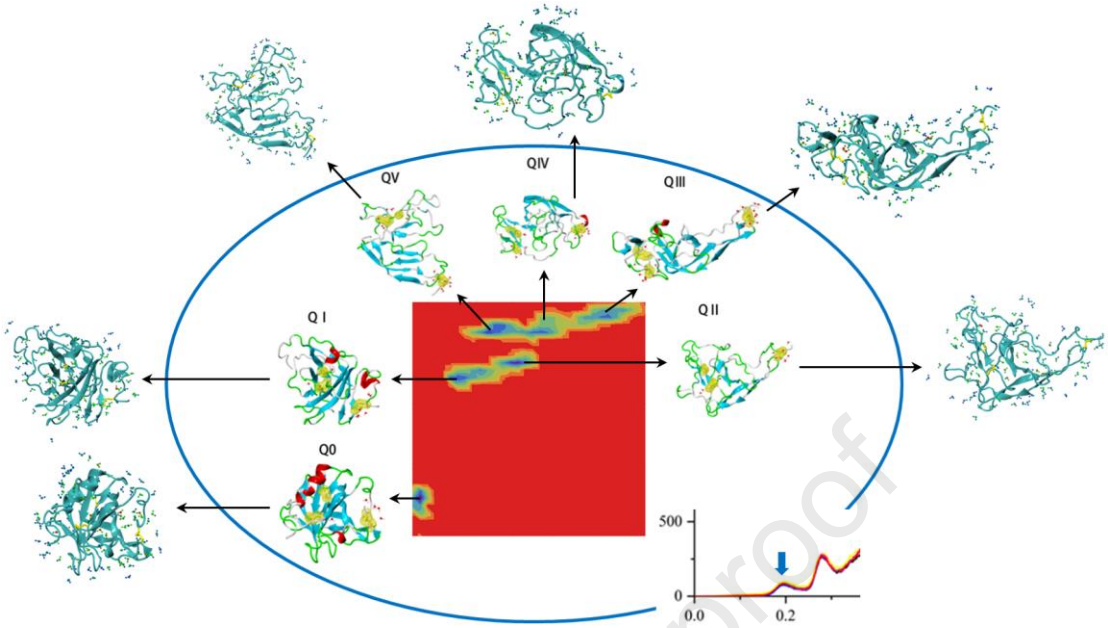

Molecular Simulation of Partially Denatured β-Lactoglobulin

Zhuo Zhang[a,b], Valeria Arrighi[c], Lydia Campbell[b,d], Julien Lonchamp[b,e] & Stephen R. Euston[f,g*]

[a]College of Food Science and Technology, Huazhong Agricultural University, Wuhan, Hubei, 430070, PR China

[b]Institute of Mechanical, Process & Energy Engineering, School of Engineering & Physical Sciences, Heriot-Watt University, Edinburgh, EH14 4AS, United Kingdom.

[c]Institute of Chemical Sciences, School of Engineering and Physical Sciences, Heriot-Watt University, Edinburgh, EH14 4AS, United Kingdom.

[d]Nandi Proteins Limited, Nine, Edinburgh Bioquarter, Lab 13, Edinburgh, EH16 4UX

[e]School of Health Sciences, Queen Margaret University, Queen Margaret University Drive, Edinburgh, EH21 6UU, United Kingdom.

[f]Institute of Biological Chemistry, Biophysics and Bioengineering, School of Engineering & Physical Sciences, Heriot-Watt University, Edinburgh, EH14 4AS, United Kingdom.

[g]Department of Physics, Toronto Metropolitan University, Toronto, Ontario, Canada.

*Corresponding author: S.R.Euston@hw.ac.uk

Abstract

The unfolding of β-lactoglobulin (β-lac) upon heating was comprehensively studied through molecular dynamics computer simulations. A β-lac molecule in the aqueous solution was firstly heated at 500 K for unfolding and then annealed at 300 K to collect stable conformations. There were five meta-stable conformations observed based on the Free Energy Landscape (FEL). The β-lac molecule was found to exhibit an open and extended conformation on heating followed by limited refolding upon cooling. The cysteine residues $–SH^{121}$ and $S–S^{66\text{-}160}$ in the most open conformation were located at the opposite ends of the β-lac molecule. This would favour the intermolecular –SH/S–S interchange reactions that are known to occur in β-lac as part of the inter-molecular aggregation process. Furthermore, the unfolding of the β-lac increased the hydrogen bond forming capacity between water molecules and the protein and between water molecules themselves. The interactions and the properties of the water molecules in the protein hydration shell also indicated that the hydration shell was stabilized by protein unfolding. However, it was found that the unfolding of β-lac increased diffusion of hydration water molecules, including those in the first hydration shell that interact more strongly with the protein. This may partly explain why unfolded proteins are more likely to aggregate even though there were more hydration water molecules protecting them. Such results provided more detailed information on the structure-functionality relationship of β-lac based on both the protein molecule and its hydration shell. This provides insight into how we can control the processing of proteins for desirable functional properties such as thickening and gelation, which are modified through protein-water interactions.

Keywords: β-lactoglobulin; denaturation; whey proteins; molecular dynamics simulation.

1. Introduction

The structure and stability of a protein molecule in solution is influenced by the way the peptide chain interacts with the solvent water molecules. It is well known that when a protein is dissolved in water, the presence of the protein solute perturbs the local hydrogen bonded structure of the water molecules. To offset this unfavourable increase in the enthalpy (and entropy) of the solvent, water molecules will interact by forming hydrogen bonds with various hydrophilic regions of the protein surface to form a "layer" of water around the molecule which is known as the hydration shell (Fogarty & Laage, 2014; Laage, Elsaesser, & Hynes, 2017). In the hydration shell, the motion of the water is slowed down compared to the bulk phase water. It is known that the degree to which the water diffusion is hindered depends on the amino acid residues close to a particular water molecule, i.e., the distribution of water diffusion coefficients within the hydration shell is not homogeneous (Russo, Murarka, Copley, & Head-Gordon, 2005). Presumably water molecules that are close to amino acid residues that interact with the water via electrostatic interactions (through charges or dipoles) will experience a greater reduction in their motion. The dynamics of this hydration shell are important in protein function in biological systems, and will also play a role in functional properties in food systems. It is a reasonable suggestion that when a globular protein molecule, such as the bovine whey protein β-lactoglobulin (β-lac), is denatured by heat, the hydration layer will be perturbed by changes to the distribution of hydrophilic groups on the protein surface and hydrophobic groups in the core, and that this may influence the way in which the protein molecules aggregate in solution. We have an ongoing

interest in understanding factors affecting the heat denaturation of proteins and their subsequent aggregation, and have investigated bovine whey proteins aggregates as functional ingredients, including as fat replacers. In our previous work we have demonstrated that controlled denaturation of β-lac solutions allows us to produce protein products with varied degrees of denaturation that have a range of rheological properties (Zhang, Arrighi, Campbell, Lonchamp, & Euston, 2016a, 2016b, 2018). The viscosity and other rheological properties of protein solutions are linked to the way in which the protein interacts with surrounding water molecules. To understand better how the structure of the denatured protein influences water mobility and interactions, we have instigated a molecular dynamics (MD) simulation study to look at the distribution of water in the hydration shell of β-lac in its native form and in five metastable partially denatured forms. Such a work would provide theoretical foundations for protein modifications in the food industry, especially in utilizations of dairy and whey proteins.

2. Methodology

All MD simulations were performed using the GROMACS 4.5 MD package (Hess, Kutzner, van der Spoel, & Lindahl, 2008). The X-ray diffraction molecular structure of bovine β-lactoglobulin A (β–lac) variant was downloaded from the Protein Data Bank (ID 3BLG) (Qin, et al., 1998). The β-lac molecule was inserted into a periodic cubic box with the sides 1.0 nm from the surface of the protein molecule in three coordinate directions. SPC water molecules (Berweger, van Gunsteren, & Müller-Plathe, 1995) were added giving a system containing 1 β-lac molecule and 11486 water molecules.

SPC water is a popular choice for MD simulations as it is reported to reproduce well the bulk phase properties at room temperature (Laage & Hynes, 2008; Stirnemann & Laage, 2012). Nine Na^+ counter ions were added to neutralize the -9e negative charge on the β-lac molecule. Since the Na+ ions are monovalent cations, they will not participate in salt bridges between acidic residues and will not contribute to intra-molecular interactions. Charge neutralization is required for efficient use of the particle-mesh-Ewald method we use for approximating long range contributions to the electrostatic interactions. The system was minimized using a steepest descent algorithm. For all the simulations, the GROMOS96 53A6 force field (Oostenbrink, Villa, Mark, & van Gunsteren, 2004) was used with electrostatic interactions modelled using the particle mesh Ewald method (Essmann et al., 1995). The system was equilibrated in the NVT ensemble at 300 K for 0.1 ns, and then in the NPT ensemble at 300 K and 1 bar for 0.1 ns. Temperature and pressure control were achieved using the velocity-rescale thermostat (Bussi, Donadio, & Parrinello, 2007) and Berendsen (Berendsen, Postma, Van Gunsteren, Di Nola, & Haak, 1984) and Parrinello-Rahman (Parrinello & Rahman, 1981) barostats during pressure equilibration and during production run, respectively. Molecular dynamics production runs were carried out at 300 K and 500 K in the NPT ensemble for 100 ns. The 500 K simulation was used to produce partially denatured conformations for further study. From the trajectory of the unfolded molecule simulated at 500 K, five metastable conformations were selected and quenched to 300 K for 102 ns to generate the partially denatured conformations. The five conformations from unfolded β-lac molecule were selected from plateaus of the root mean square deviation

(RMSD) of the backbone of the unfolded molecule with respect to the native conformation (Figure 1). The plateaus correspond to time sequences where the RMSD of the protein changes little and therefore is likely to be a metastable state. RMSD is calculated from the atomic coordinates of the unfolded molecule, $\mathbf{r}_{it}$, and of the reference the native β-lac molecule, $\mathbf{r}_{i0}$,

$$RMSD = \sum_{i=1}^{N} \left(\mathbf{r}_{it} - \mathbf{r}_{i0} \right)^2 \qquad (1)$$

At the end of the simulations, six different β-lac conformations were obtained at 300 K, i.e., one native and five unfolded β-lac molecules with different conformations. The first 3 ns of the trajectories were discarded for further analyses on the five unfolded β-lac conformations as these correspond to the time required for the temperature to reduce to 300K. Thus, the analyses for the quenched conformations were applied based on the last 99 ns of the trajectory.

Free energy landscapes (FEL) were calculated to find the representative structures for each of the six conformations, and these were used for further analyses. For the FEL, two parameters are used as conformational markers to distinguish between molecular conformations, i.e., two conformations of a protein are considered identical if they have the same values of the conformational markers. This is an approximation that is sufficiently accurate for free energy determination (Maisuradze, Liwo, & Scheraga, 2009, 2010). In practice, the radius of gyration (R_g) and the root mean square deviation ($RMSD$) of the protein molecule are usually selected as the two conformational markers, and these parameters were also used in this work. From the population of the conformations for each paired parameters, $P_i(R_g, RMSD)$, the thermodynamic potential

ψ is obtained as,

$$G_{Gibbs}\left(R_g, RMSD\right) = -k_B T \ln P_i\left(R_g, RMSD\right) \qquad (2)$$

where k_B and T are the Boltzmann constant and the absolute temperature, respectively. The Gibbs free energy, G_{Gibbs}, is defined as the thermodynamic potential in the isothermal-isobaric (*NPT*) ensemble, and therefore, the FEL of the simulations is equivalent of the G_{Gibbs} as a function of a pair of structural parameters. Finally, the structure of each molecule was represented by the conformation with the lowest Gibbs free energy. The calculations of diffusion coefficients and mobilities of water molecules in the hydration shells were carried out on the representative structure and their subsequent trajectories.

The volumetric number densities of water molecules around the proteins were calculated. The number of the oxygen atoms of water molecules was counted as a function of the distance (d) from the protein surface, giving the number distribution of water molecules ($N_d[H_2O]$). Since the surface distribution function ($N_d[H_2O]$) was not normalized and only gives the number of the water molecules, the number density of water molecules within the distance d from the protein surface, $\rho_d[H_2O]$, was introduced to eliminate the effects of the available room that increased with d (as shown in Scheme 1). A series of probes (r) ranging from 0 to 0.998 nm with an increment (δ) of 0.002 nm were applied to calculate the volumes of the protein molecules (V_r). Therefore, the volume of a shell with the thickness of δ and the distance d from the protein surface, $V_{\delta|r=d}$, was obtained.

$$V_{\delta|r=d} = V_d - V_{(d-\delta)} \qquad (3)$$

Since $N_d[H_2O]$ was counted as d increased by δ=0.002 nm, the number density of water molecules, $\rho_d[H_2O]$, with the distance d from the protein surface can be defined as,

$$\rho_d\left[H_2O\right] = \frac{N_d\left[H_2O\right]}{V_{\delta|r=d}} \qquad (4)$$

The number of hydrogen bonds (HB) formed between water molecules in the hydration shell, bulk water molecules and between water molecules in the hydration shell and the protein molecule were counted. In GROMACS, a hydrogen bond is defined based on a geometrical criterion where the distance between the hydrogen (H) and the acceptor (A) must be smaller than 0.35 nm and the angle of donor-hydrogen-acceptor (ADH) must be smaller than 30°. The protein-water (PW) and water-water (WW) HB forming capacities of the hydration water molecules, $C[HB]_{PW}$ and $C[HB]_{WW}$ are expressed as,

$$C\left[HB\right]_{PW|shell} = \frac{N\left[HB\right]_{PW|shell}}{N\left[H_2O\right]_{shell}} \qquad (5)$$

and

$$C\left[HB\right]_{WW|shell} = \frac{N\left[HB\right]_{WW|shell}}{N\left[H_2O\right]_{shell}} \qquad (6)$$

where N denotes the number of HB or H_2O molecules and shell indicates the locations of the water molecules in the hydration shells.

Weak interactions including van der Waals interactions and hydrogen bonds between the water molecules in the individual hydration shells and between water and the protein were evaluated according to the independent gradient model (IGM) (Lefebvre, Rubez,

Khartabil, Boisson, Contreras-García, & Hénon, 2017). When atoms approach and interact with each other, their electron density gradients ($\nabla\rho(\mathbf{r})$) exhibit opposite monotonicities in the space between them and therefore the absolute sum of those electron density gradients, $\left|\sum_i \nabla\rho_i(\mathbf{r})\right|$, decreases in such space. In the IGM method, the absolute electron density gradients of the individual atoms are summed (i.e., $\sum_i |\nabla\rho_i(\mathbf{r})|$) and the difference between $\sum_i |\nabla\rho_i(\mathbf{r})|$ and $\left|\sum_i \nabla\rho_i(\mathbf{r})\right|$ is employed to evaluate the interactions between atoms. The descriptor δg_{inter} proportional to the non-covalent interactions between molecules was further introduced for multi-molecular systems.

$$\delta g_{\text{inter}} = \left|\sum_M \left|\sum_{i\in M} \nabla\rho_i(\mathbf{r})\right|\right| - \left|\sum_M \sum_{i\in M} \nabla\rho_i(\mathbf{r})\right| \qquad (7)$$

where $\sum_{i\in M}$ and $\sum_M$ indicated summations within each molecule and between all the molecules in the system, respectively. In practice, the representative structures were employed and the atomic contributions to the spatial δg_{inter} of each molecule were calculated with the Multiwfn 3.6 software package (Lu & Chen, 2012).

The diffusion coefficient of water molecules in the hydration shells around the proteins were also evaluated based on the representative structures and their subsequent trajectories. The diffusion coefficient was calculated for each water molecule from the mean square displacement (using the g_msd tool in GROMACS) and the diffusion coefficients for individual hydration shells were obtained. Additionally, another box of 3×3×3 nm^3 containing 884 water molecules was built for determination of the diffusion coefficient of the bulk water using the same methdology. The forcefield (GROMOS96

53A6), water model (SPC), thermostat (velocity-rescale) and barostats (Berendsen for pressure equilibration and Parrinello-Rahman for production run) were the same as those employed for protein simulations. The only difference was that no heating procedure was introduced and 1 ns of simulation was applied for water rather than 100 ns at 300 K.

3. Results & Discussion

3.1 Conformations of β-lactoglobulin

It is well known that protein molecules unfold and lose their tertiary structures under heat treatment. The extent of heat-induced denaturation of a protein molecule can be followed in simulated systems using the *RMSD* of the backbone of unfolded polypeptides relative to the native protein structure. Earlier simulations have demonstrated that globular proteins simulated at high temperature unfolded in a series of stages (Day, Bennion, Ham, & Daggett, 2002; Euston, 2013; Euston, Ur-Rehman, & Costello, 2007). This is characterized by the protein passing through a series of partially unfolded metastable states. It was also established that protein heat denaturation simulated at high temperature (500 K) follows the same pathway, albeit at a faster rate, as denaturation does at 350 K. It has been observed experimentally that below 58 ºC reversible changes occur in the tertiary fold of β-lac, but the secondary structure is conserved. Above 58 ºC changes to conformation become irreversible, with a rapid loss of α-helix at 65 ºC and changes observed in the β-sheet (Qi, Brownlow, Holt, & Sellers, 1995; Qi, Holt, McNulty, Clarke, Brownlow, & Jones, 1997).

The RMSD of a simulated β-lac molecule in water at high temperature (500 K) is

plotted together with the RMSD at 300 K in Figure 1. Fluctuations of the RMSD of the molecule at 300 K were a result of molecular vibration of the protein (Zhang, Hu, Xu, Pan, & Peng, 2019). In a previous simulation paper (Euston, 2013), we showed that unfolding of β-lac proceeded via excitation of various collective modes of motion, which involved correlated motions of groups of residues within the structure. Initially, it appears that amino acid residues in the loops at the ends of β-strands are excited and these propagate down the β-sheets leading to their disruption. In the same paper we also reported that during heating at 500 K the β-lac unfolds via at least two intermediate metastable conformations. The changes in RMSD observed in our earlier paper are broadly in agreement with the results observed here. Stepwise heat-induced unfolding of the β-lac molecule is observed in Figure 1, where the protein unfolds via several metastable states. We have identified five unfolded states, marked in Figure 1, which appear to be transiently stable before unfolding further. These five conformations were used to generate five partially unfolded states of the β-lac molecule by quench cooling the conformations to 300 K and simulating these for a further 100 ns. The RMSD of the annealed molecules (denoted QI - QV) are shown in Figure 2 and compared to the native conformation RMSD (QO). The RMSD for the five partially denatured states remained high on cooling indicating that refolding to the native structure does not take place. Compared with the protein heated at 500 K in Figure 1, the annealed molecules exhibited small fluctuations in RMSD, indicating that these molecules preserved their meta-stable structures from further unfolding at room temperature. The Gibbs free energy of each protein molecule was calculated and plotted as a free energy landscape

(FEL) (Figure 3a). According to the FEL, the heated protein molecules (i.e., QI - QV) explore further unfolded conformations when quench cooled. The FEL can be used to find representative structure for the partially unfolded conformations. These correspond to the conformations with the lowest Gibbs free energies for the different partially unfolded proteins. From Figure 3a it is clear that the β-lac molecule experienced at least a two-step phase transition upon heating. There were two continuous pathways, i.e., QI to QII and QIII to QV. Moreover, it was interesting to find that the conformation QIII exhibited the most extensive structure i.e., its energy landscape was larger. We surmised that further unfolding of the QIII conformation provided more hydrophobicity and flexibility to the molecule and resulted in refolding of the polypeptide into alternative conformations close together in energy.

Representative structures of the quenched molecules obtained from FELs are shown in Figure 3b. β-lac has five cysteine (Cys) residues in the polypeptide chain, of which four are connected by two disulphide bonds, i.e., S–S$^{66\text{-}160}$ and S–S$^{106\text{-}119}$. The sulphydryl group of Cys^{121} is a free SH group. The disulphide bonds play a key role in maintaining structure in the β-lac molecules. In Figure 3b (the native state structure, QO), S–S$^{106\text{-}119}$ joins two β-sheet regions and helps to stabilise the β-barrel lipid binding pocket. The other disulphide bond, S–S$^{66\text{-}160}$, on the other hand joins another β-sheet region to the C-terminal end of the peptide chain, and thus helps to maintain the compact globular conformation of β-lac. In Figure 3b (conformation QI) there was significant loss of α-helix, whilst most of the β-sheet remained intact due in part to the stabilising effect of S–S$^{106\text{-}119}$, although the β-barrel structure started to become less distinct. The S–S$^{66\text{-}160}$

disulphide bond had greater opportunity for flexibility and moved further from its position in the native state. As heating continued through QII-QV there was further loss of α-helix, and further loss of definition of the β-barrel, although the individual β-sheets were relatively intact even for conformation QV which had been heated at 500K for the longest time. The loss of the tertiary fold during heating released Cys residues from β-sheets into more flexible structures, such as coils and turns. From the conformations in Figure 3b it was apparent that the major structural changes during the heating of the β-lac were in the tertiary fold. The structural changes observed for the β-lac molecule during the early stages of heating are characteristic of a transition to a molten globule state, which has been reported previously for β-lac (Carrotta, Bauer, Waninge, & Rischel, 2001; Qi et al., 1995; Qi et al., 1997). A molten globule conformation is described as having an expanded tertiary fold, exposed hydrophobic residues, increased dynamic accessibility of the amide bond, absence of cooperativity in heat denaturation and increased protein aggregation (Hirose, 1993). More recently, the concept of the molten globule has been refined to account for the observation that it is possible to form a dry molten globule, where the tertiary fold is loosened but water does not penetrate the interior of the globule, and a wet molten globule where the hydration layer extends into the loosened hydrophobic core of the molecule (Bhattacharyya & Varadarajan, 2013). In these simulations if a molten globule was formed it was likely to be in the QI conformation, since the secondary structure changes from QII to QV were more extensive than might be expected for the molten globule. It was also observed in Figure 3b that $–SH^{121}$ and $S–S^{106\text{-}119}$ were distributed on the opposite ends of the unfolded

protein molecules to S–S[66-160]. These locations of the free –SH[121] and S–S bonds and the flexibility of the unfolded structures could favour the intermolecular SH/S–S interchange reactions that are important in aggregation reactions (Shimada & Cheftel, 1989). We should emphasise here that when β-lac is heated experimentally, there is the possibility of breakage and reorganisation of the S–S bonds (thiol interchange reactions). In contract, the S–S bonds remain intact in the molecular dynamics simulations, as there is no mechanism to allow for them to break using standard force fields.

3.2 Hydration Shells of β-lactoglobulin

In addition to changes in the tertiary and secondary structures, unfolded proteins also modify their hydration shells outside the molecular surfaces. It is believed that hydration waters have very distinct behaviour from bulk water, since the former interact directly with the protein or their interactions with other water molecules are affected by the protein molecular surface (Ball, 2008). It has been concluded that water molecules form H-bonds directly with polar amino acid groups when they are close, while those close to nonpolar amino acid groups will preferentially H-bond with other water molecules (Raschke, 2006; Russo et al., 2005). This leads to a slowing of the dynamics of the protein bound water.

The water distributions around the surfaces of the different protein molecules were expressed as the number density of water molecules ($\rho_d[H_2O]$ from the protein surface as shown in equation 4. It was found that $\rho_d[H_2O]$ increased with the distance (d) from

the protein surface (Figure 4), regardless of the unfolding extent of the proteins. The data for $\rho_d[H_2O]$ in Figure 4 suggests three hydration shells around the protein molecules, with the distances of 0.24 nm (shell 1), 0.24~0.32 nm (shell 2) and 0.32~0.53 nm (shell 3) from the protein surface, respectively. The different hydration shells will correspond to differing degrees or strengths of binding to the protein, with the third hydration shell having a more diffuse structure that forms a transition region between bound water and bulk water. The thickness of those hydration shells was found to be independent of the protein conformations with QO-QV, all exhibiting very similar distance dependence. The QIII β-lac conformation was observed to have the densest hydration shells. Moreover, it seemed that some water molecules penetrated the QIII protein surface since its first hydration shell started very close to the protein surface, even from 0.05 nm. As shown in Figure 1, the QIII conformation had the highest R_g and *RMSD* of all the conformations and thus had a more open structure that was more easily accessible to hydration water molecules. Such an open structure favours water penetration and more solvent accessible residues would also improve the interactions between the protein and water molecules as well as the interactions between the water molecules themselves, together giving a dense packing of water molecules in the hydration shells.

3.3 Hydrogen Bonds in Hydration Shells of β-lactoglobulin

Since water molecules in the hydration shells of a protein can from hydrogen bonds either with the protein surface or with themselves, analyses of the hydrogen bonding capacities of water molecules can also reveal how the hydration shells respond to

protein unfolding. The hydrogen bond (HB) forming capacities of the hydration water molecules, $C[HB]_{TOT}$, were expressed as the sum of the protein-water and water-water HB forming capacities (i.e., $C[HB]_{PW}$ and $C[HB]_{WW}$ as shown in equations 5 and 6, respectively) and are plotted in Figure 5a. It was found that protein unfolding exerted different effects on the HB forming capacities of hydration water molecules in the individual shells. The largest $C[HB]_{TOT}$ were found for the hydration shell 1, which is likely to result from the large contributions from $C[HB]_{PW|1}$. For the same reason, $C[HB]_{TOT}$ for the hydration shell 2 were also larger than those for hydration shell 3. On the other hand, however, protein unfolding had inconsistent effects on $C[HB]_{TOT}$ except for shell 1. Such observations would result from the various effects of protein unfolding on the protein-water and water-water (including intra-shell and inter-shell) HB forming capacities for the individual hydration shells. The protein-water HB forming capacities, $C[HB]_{PW}$, were plotted in Figure 5b. It was found that water molecules in the hydration shell 1 had a greater tendency to form hydrogen bonds with the protein ($C[HB]_{PW|1}$) than those in the hydration shell 2 and shell 3. Since the water molecules in the hydration shell 3 were so far from the protein surface (0.32~0.53 nm), it was rational to find very small values for $C[HB]_{PW|3}$. Additionally, the fact that the O atoms of water molecules in the hydration shell 1 were closer to the protein surface than those in the hydration shell 2 explained the difference between $C[HB]_{PW|1}$ and $C[HB]_{PW|2}$, since O atoms were more capable of forming HB than H atoms. It was interesting to find that the most open two conformations, i.e., QIII and QV conformations exerted very limited effect on protein-water HB. There was also no significant increase in $C[HB]_{PW|1}$ for the

QV conformation. Furthermore, unfolding of β-lac even decreased $C[HB]_{PW|2}$. It seemed that the protein unfolding disrupted the favourable molecular surface for protein-water HB.

The water-water HB forming capacities ($C[HB]_{WW}$) of water molecules in the hydration shells are shown in Figure 5c. It was found that the water molecules in the same hydration shell were more inclined to form hydrogen bonds with each other than those in the bulk water. Moreover, those water molecules in the hydration shells further from the protein surface preferred water-water HB rather than water-protein HB. It seemed that QIII and QV protein conformations promoted water-water H-bonding, especially in the first and second shells. Such observations in $C[HB]_{WW}$ were contrary to those in $C[HB]_{PW}$ and it seemed that a water molecule tended to form HB with either the protein molecule or the other water molecule(s) but seldom with both. To understand the detailed responses of water molecules to protein unfolding, $C[HB]_{WW}$ were further decomposed into water-water HB forming capacities within the hydration shells ($C[HB]_{WW|shell}$) and between different hydration shells/bulk ($C[HB]_{WW|shell\text{-}shell/bulk}$) as shown in Figure 5d to Figure 5f. The bulk water had the largest water-water HB forming capacities with each other while those inside shell 1 had the smallest water-water HB forming capacities, which again suggests that hydrogen bonding with the protein perturbed water-water HB formation. Moreover, protein unfolding tended to increase the intra-shell HB formations for water molecules in shell 1 and shell 2 while such effects were not so significant for those in shell 3. It was noted that the water molecules in hydration shell 1 preferred forming water-water HB with those in other hydration

shells, especially in shell 3. As mentioned before, GROMACS counts HB geometrically. The largest distance between a hydrogen atom and an acceptor for an HB can reach 0.35 nm while the thickness of the hydration shell 2 was around 0.08 nm. Thus, it is not surprising to find water-water HB between hydration shell 1 and hydration shell 3. Similar findings were observed for the water molecules in hydration shell 2, where the molecules tended to form HB with those in shell 3. As for those water molecules in shell 3, they prefer hydrogen bonds with the bulk water and themselves rather than those in shell 2 and shell 1. Since the thickness of hydration shell 3 was much larger than that of shell 1 or shell 2, such results are due to the large distance of most water molecules in shell 3 from those in shell 1 and shell 2. The inter-shell HB formations were also affected by protein unfolding. It was observed that $C[HB]_{WW|1\text{-}2}$, $C[HB]_{WW|2\text{-}1}$, $C[HB]_{WW|2\text{-}3}$, $C[HB]_{WW|2\text{-}bulk}$ and $C[HB]_{WW|3\text{-}2}$ were increased by protein unfolding, especially those for QIII and QV conformations, indicating that the distributions and orientations of the hydration water molecules were influenced by protein structure and therefore the HB formations were altered. From Figure 5, it was found that the hydration water molecules in shell 1 and shell 2 preferred to form HB with the protein and water molecules in shell 3 while those in shell 3 had larger HB forming capacities for the bulk water and themselves. Therefore, the hydration water molecules in shell 1 and shell 2 exhibit more hydration behaviour but differ in orientations, while those in shell 3 act as a transition region between hydration water and bulk water.

3.4 Distributions and Interactions of Hydration Water around β-lactoglobulin

Other than hydrogen bonds, non-covalent interactions such as van der Waals forces also

401 exist between water molecules and the protein, as well as between the water molecules
402 themselves. To understand the weak interactions (including hydrogen bonding) more
403 specifically, the independent gradient model (IGM) was employed and the values of
404 δg_{inter} were calculated following equation 7. Figure 6 illustrates quantitatively the
405 interactions of hydration water in each shell with the β-lac molecule based on the value
406 of δg_{inter} for each atom in a water molecule. It was found that those water molecules in
407 the first hydration shell interacted with the β-lac dominantly through their oxygen atoms
408 as suggested by their large δg_{inter} values, while the water molecules in the second
409 hydration shell preferred interacting with the β-lac molecule through hydrogen atoms.
410 It was not surprising that there were very few water molecules in the third hydration
411 shell interacting with the protein molecule since the shortest distance (0.32 nm) between
412 the layer and β-lac was very close to the maximal length of hydrogen bonds (0.35 nm).
413 As β-lac was unfolded, more water molecules in the hydration shells, especially those
414 in the first and second shells, were found to interact with the protein molecule, resulting
415 from the increased flexibility and the solvent accessible surface of the protein.
416 Moreover, it was also found that those unfolded β-lac conformations, especially those
417 with extensive structural changes (i.e. QII and QIII) exhibited stronger interactions with
418 their hydration water. The results seemed to contradict the observations of hydrogen
419 bonding between the hydration water molecules and the unfolded protein. However, we
420 should bear in mind that the hydrogen bonds were defined geometrically while the
421 interactions between the water molecules and the proteins were determined through
422 IGM and contained van der Waals interactions in addition to hydrogen bonds. The

interactions between water molecules in different hydration shells are also explored based on δg_{inter} values as illustrated in Figure 7. Similar to the observations in Figure 6, it was found that the unfolding of the protein improved the interactions between the hydration shells, especially for conformations QII and QIII. Moreover, the interactions between water molecules in shell 2 and shell 3 were predominant, consistent with the fact that the water in shell 1 preferred interacting with the protein molecule. Such results confirmed that unfolding of protein enhanced the interactions between water molecules and the protein.

3.5 Diffusion Coefficient and Mobility of Water around β-lactoglobulin

It is well known that the functionalities such as viscosity of a protein solution would be influenced once the protein unfolds. Changes in the viscosity of a protein solution (thickening) on heating occur due to changes in the mobility of water molecules promoted by the unfolding of the protein structure. To follow this, we calculated the diffusion coefficient of the hydration water molecules around QO to QV β-lac conformations, as well as that of the bulk water. The values of the diffusion coefficients of the water molecules in different hydration shells and in the bulk are listed in Table 1. It was found that the diffusion coefficient of the bulk water from our simulation ($2.81\pm0.17 \times 10^{-5}$ cm^2s^{-1}) was very close to the reference values (2.30 to 2.62×10^{-5} cm^2s^{-1} from 298 K to 303 K) (Holz, Heil, & Sacco, 2000; Tofts et al., 2000). However, the diffusion coefficients for those hydration water molecules were much smaller than that of the bulk, and the values (from 1.10 ± 0.64 to $1.87\pm1.12 \times 10^{-5}$ cm^2s^{-1}) were comparable with those of the bulk water at around 273 K to 288 K (1.13 to 1.77×10^{-5} cm^2s^{-1})

445 (Easteal, Price, & Woolf, 1989; Holz et al., 2000). It was also noted that β-lac also
446 exerted influence on the hydration water molecules in shell 3, even though such a shell
447 was far from the protein surface and acted as a transition region between hydration and
448 bulk waters. Moreover, diffusions of hydration water molecules were altered by
449 unfolding of β-lac according to Table 1. The most extended QIII conformation of β-lac
450 had the largest increasing effects on the diffusion coefficients of the hydration water
451 molecules. Since unfolded protein conformations enhanced the interactions between
452 hydration water molecules themselves due to the hydrophobic effects, which would
453 accelerate the exchanges of water molecules between hydration shells. More
454 importantly, the increased hydrophobic effects from β-lac unfolding also raised the
455 diffusion coefficient of the hydration shell 1, where the water molecules interacted
456 mainly with the protein.

457 **4. Conclusion**

458 Heat-induced denaturation of the β-lactoglobulin (β-lac) was comprehensively studied
459 through molecular dynamics computer simulations. The β-lac was found to unfold in a
460 series of stages upon heating and five meta-stable conformations during unfolding were
461 observed based on the Free Energy Landscape (FEL). It was interesting to find that the
462 β-lac molecule experienced some refolding stages under extreme heating for a long
463 time after a very open and extended conformation. For the most open conformation (i.e.
464 QIII in the current study), the $–SH^{121}$ and $S–S^{66\text{-}160}$ were located at the opposite ends of
465 the unfolded β-lac, providing the prerequisite for intermolecular SH/S–S interchange
466 reactions and the formation of linear, fibrillar aggregates (Bryant & McClements, 1998).

Moreover, unfolding of the β-lac was found to increase the hydrogen bond forming capacity of water molecules with the protein and themselves. Further quantitative studies on the interactions and the properties of the hydration water molecules confirmed that the hydration shells were actually stabilized by protein unfolding. Since more open conformations brought higher hydrophobicity, it was understandable that the unfolded β-lac enhanced the interactions between water molecules themselves through hydrophobic effects. Such enhanced water-water interactions were found to increase the diffusion coefficients of water molecules in the hydration shells. It was interesting to find that the diffusion of water molecules in the hydration shell 1 was also increased upon protein unfolding, which may explain why the extended conformation of a protein is more likely to aggregate even though it possessed more hydration water molecules.

It should be noted that the results for water dynamics and distribution may depend partly on the water model used for the simulations. Here we chose SPC/E water, which is the preferred model for the GROMOS suite of force fields, although other water models are available. SPC has been demonstrated to reproduce the room temperature bulk phase properties of water (Laage & Hynes, 2008; Stirnemann & Laage,2012). Other researchers have compared SPC/E and TIP3P water models for their ability to reproduce water dynamics in hydration shells. Tarek & Tobias (2000) have shown that the structure of ribonuclease A differs little between simulations where SPC/E and TIP3P water are used. Comparison of simulated results with neutron scattering data for suggests that SPC/E reproduces better the water dynamics due to perturbation by the protein structure over a wide range of frequencies and temperatures (Tarek & Tobias,

2000). Thus, SPC/E water is a suitable water model choice for the studies here.

The current research could be of value in understanding the functionality of proteins under various processing conditions, in the food and the protein industry, and for section of various conditions to alter such properties.

Acknowledgements

SRE acknowledges Heriot-Watt University for the award of a PhD Scholarship to Zhuo Zhang and the Engineering & Physical Sciences Research Council for grant No. EP/J501682/1.

References

Ball, P. (2008). Water as an active constituent in cell biology. *Chemical Reviews, 108*(1), 74-108.

Berendsen, H. J. C., Postma, J. P. M., Van Gunsteren, W. F., Di Nola, A., & Haak, J. R. (1984). Molecular dynamics with coupling to an external bath. *Journal of Physical Chemistry, 81*(8), 3684-3690.

Berweger, C. D., van Gunsteren, W. F., & Müller-Plathe, F. (1995). Force field parametrization by weak coupling. Re-engineering SPC water. *Chemical Physics Letters, 232*(5-6), 429-436.

Bhattacharyya, S., & Varadarajan, R. (2013). Packing in molten globules and native states. *Current Opinion in Structural Biology, 23*, 11-21.

Bryant, C. M., & McClements, D. J. (1998). Molecular basis of protein functionality with special consideration of cold-set gels derived from heat-denatured whey. *Trends in Food Science and Technology, 9*(4), 143-151.

Bussi, G., Donadio, D., & Parrinello, M. (2007). Canonical sampling through velocity rescaling. *Journal of Chemical Physics, 126*(1), 014101(014101-014107).

Carrotta, R., Bauer, R., Waninge, R., & Rischel, C. (2001). Conformational characterization of oligomeric intermediates and aggregates in β-lactoglobulin heat aggregation. *Protein Science, 10*(7), 1312-1318.

Day, R., Bennion, B. J., Ham, S., & Daggett, V. (2002). Increasing temperature accelerates protein unfolding without changing the pathway of unfolding. *Journal of Molecular Biology, 322*(1), 189-203.

Easteal, A. J., Price, W. E., & Woolf, L. A. (1989). Diaphragm cell for high-temperature diffusion measurements. *Journal of the Chemical Society: Faraday Transactions 1, 85*(5), 1091–1097. https://doi.org/DOI:10.1039/F19898501091.

Essmann, U., Perera, L., Berkowitz, M. L., Darden, T., Lee, H., & Pedersen, L. G. (1995). A smooth particle mesh Ewald method. *Journal of Chemical Physics, 103*(19), 8577-8593.

Euston, S. R. (2013). Molecular dynamics simulation of the effect of heat on the conformation of bovine β-lactoglobulin A: A comparison of conventional and accelerated methods. *Food Hydrocolloids, 30*(2), 519-530. https://doi.org/10.1016/j.foodhyd.2012.07.016.

Euston, S. R., Ur-Rehman, S., & Costello, G. (2007). Denaturation and aggregation of b-lactoglobulin - a preliminary molecular dynamics study. *Food Hydrocolloids, 21*(7), 1081-1091.

Fogarty, A. C., & Laage, D. (2014). Water dynamics in protein hydration shells: The molecular origins of the dynamical perturbation. *Journal of Physical Chemistry B, 118, ,* (28), 7715-7729.

Hess, B., Kutzner, C., van der Spoel, D., & Lindahl, E. (2008). Gromacs 4: Algorithms for highly efficient, load-balanced, and scalable molecular simulation. *Journal of Chemical Theory and Computation, 4*(3), 435-477.

Hirose, M. (1993). Molten globule state of food proteins. *Trends in Food Science & Technology, 4*(2), 48-51.

Holz, M., Heil, S. R., & Sacco, A. (2000). Temperature-dependent self-diffusion coefficients of water and six selected molecular liquids for calibration in accurate ^{1}H NMR PFG measurements. *Physical Chemistry Chemical Physics, 2*, 4740–4742. https://doi.org/DOI: 10.1039/B005319H.

Laage, D. & Hynes, J. T. (2008). On the Molecular Mechanism of Water Reorientation. Journal of Physical Chemistry B, 112, 14230−14242.

Laage, D., Elsaesser, T., & Hynes, J. T. (2017). Water dynamics in the hydration shells of biomolecules. *Chemical Reviews, 117*, 10694-10725.

Lefebvre, C., Rubez, G., Khartabil, H., Boisson, J.-C., Contreras-García, J., & Hénon, E. (2017). Accurately extracting the signature of intermolecular interactions present in the NCI plot of the reduced density gradient versus electron density. *Physical Chemistry Chemical Physics, 19*(27), 17928-17936.

Lu, T., & Chen, F. (2012). Multiwfn: A multifunctional wavefunction analyzer. *Journal of Computational Chemistry, 33*(5), 580-592.

Maisuradze, G. G., Liwo, A., & Scheraga, H. A. (2009). Principal component analysis for protein folding dynamics. *Journal of Molecular Biology, 385*(1), 312-329.

Maisuradze, G. G., Liwo, A., & Scheraga, H. A. (2010). Relation between free energy landscapes of proteins and dynamics. *Journal of Chemical Theory and Computation, 6*(2), 583-595.

Oostenbrink, C., Villa, A., Mark, A. E., & van Gunsteren, W. F. (2004). A biomolecular force field based on the free enthalpy of hydration and solvation: The GROMOS force-field parameter sets 53A5 and 53A6. *Journal of Computational Chemistry, 25*(13), 1656-1676.

Parrinello, M., & Rahman, A. (1981). Polymorphic transitions in single crystals: a new molecular dynamics method. *Journal of Applied Physics, 52*(12), 7182-7190.

Qi, X. L., Brownlow, S., Holt, C., & Sellers, P. (1995). Thermal denaturation of β-

lactoglobulin: effect of protein concentration at pH 6.75 and 8.05. *Biochimica et Biophysica Acta, 1248*(1), 43-49.

Qi, X. L., Holt, C., McNulty, D., Clarke, D. T., Brownlow, S., & Jones, G. R. (1997). Effect of temperature on the secondary structure of beta-lactoglobulin at ph 6.7, as determined by cd and ir spectroscopy: A test of the molten globule hypothesis. *Biochemical Journal, 324*(Pt 1), 341-346.

Qin, B. Y., Bewley, M. C., Creamer, L. K., Baker, H. M., Baker, E. N., & Jameson, G. B. (1998). Structural basis of the tanford transition of bovine β-lactoglobulin. *Biochemistry, 37*(40), 14014-14023.

Raschke, T. M. (2006). Water structure and interactions with protein surfaces. *Current Opinion in Structural Biology, 16*(2), 152-159.

Russo, D., Murarka, R. K., Copley, J. R., & Head-Gordon, T. (2005). Molecular view of water dynamics near model peptides. *Journal of Physical Chemistry B, 109*(26), 12966-12975.

Shimada, K., & Cheftel, J. C. (1989). Sulfhydryl group/disulfide bond interchange reactions during heat-induced gelation of whey protein isolate. *Journal of Agricultural and Food Chemistry, 37*(1), 161-168.

Stirnemann, G., & Laage, D. (2012). On the origin of the non-Arrhenius behavior in water reorientation dynamics. Journal of Chemical Physics, 137, 031101.

Tarek, M. & Tobias, D. J. (2000). The dynamics of protein hydration water: a quantitative comparison of molecular dynamics simulations and neutron-scattering experiments. Biophysical Journal, 79, 3244-3257.

Tofts, P. S., Lloyd, D., Clark, C. A., Barker, G. J., Parker, G. J. M., McConville, P., . . . Pope, J. M. (2000). Test liquids for quantitative MRI measurements of self-diffusion coefficient in vivo. *Magnetic Resonance in Medicine, 43*(3), 368–374. https://doi.org/DOI: 10.1002/(SICI)1522-2594(200003)43:3<368::AID-MRM8>3.0.CO;2-B.

Zhang, Z., Arrighi, V., Campbell, L., Lonchamp, J., & Euston, S. R. (2016a). Properties of partially denatured whey protein products 2: Solution flow properties. *Food Hydrocolloids, 56*, 218-226.

Zhang, Z., Arrighi, V., Campbell, L., Lonchamp, J., & Euston, S. R. (2016b). Properties of partially denatured whey protein products: Formation and characterisation of structure. *Food Hydrocolloids, 52*, 95-105.

Zhang, Z., Arrighi, V., Campbell, L., Lonchamp, J., & Euston, S. R. (2018). Properties of partially denatured whey protein products: Viscoelastic properties. *Food Hydrocolloids, 80*, 298-308.

Zhang, Z., Hu, H., Xu, X., Pan, S., & Peng, B. (2019). Insights of Pressure-induced Unfolding of β-Lactoglobulin as Revealed by Steered Molecular Dynamics. *Advanced Theory and Simulations, 2*, 1800199. https://doi.org/10.1002/adts.201800199.

609

610 **Table 1**. Diffusion coefficients of water in the individual hydration shells of various β-
611 lac conformations and in the bulk.

Conformation	Water Diffusion Coefficient in Hydration Shell ($\times 10^{-5}$ cm^2s^{-1})			
	Shell 1	Shell 2	Shell 3	Bulk
QO	1.25±0.73	1.39±0.71	1.47±0.81	2.81±0.17
QI	1.10±0.64	1.29±0.66	1.34±0.68	
QII	1.28±0.86	1.42±0.91	1.55±0.98	
QIII	1.62±1.04	1.79±1.04	1.87±1.12	
QIV	1.47±0.88	1.56±0.92	1.61±0.93	
QV	1.39±0.91	1.60±0.97	1.68±0.96	

612

613

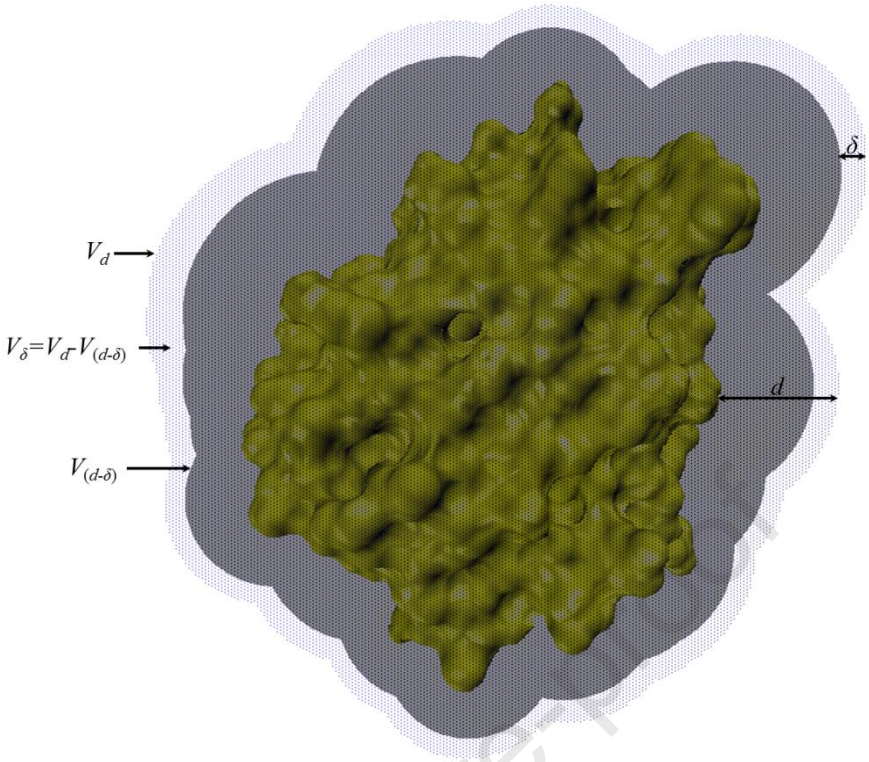

614

615

616 **Scheme 1.** Illustration of the volume of a shell with the thickness of δ and the distance

617 d from the protein surface ($V_{\delta|r=d}$).

618

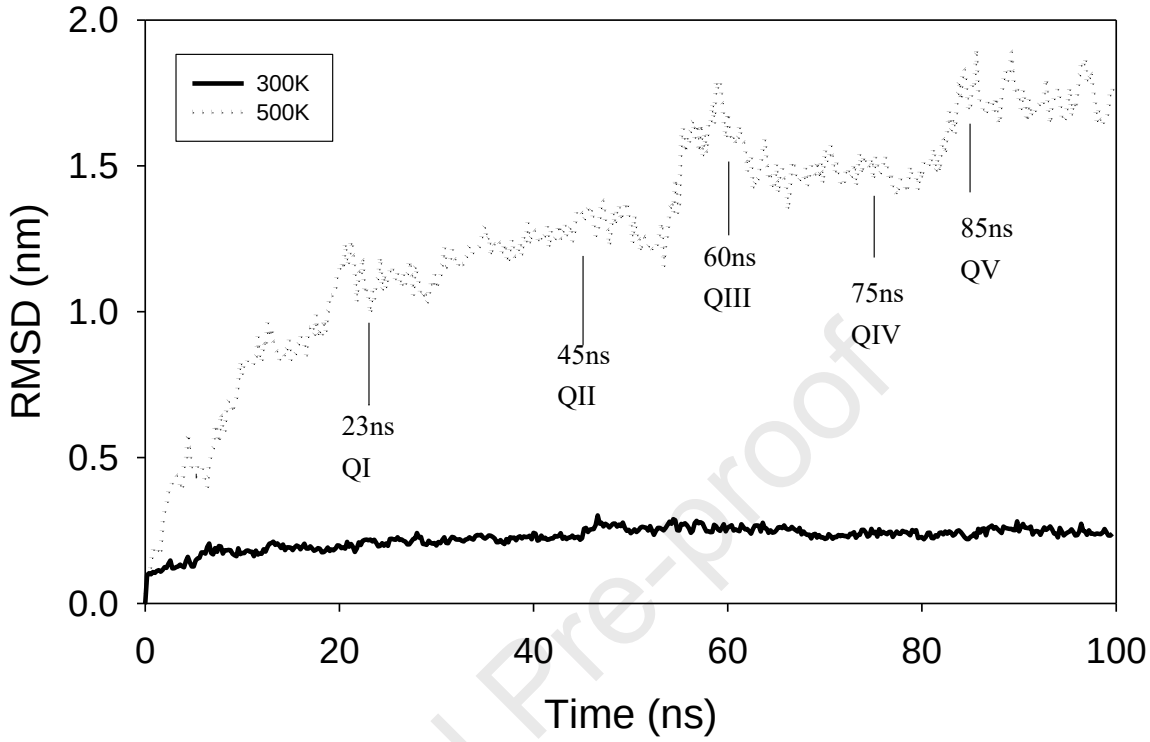

619

620 **Figure 1.** Root mean square deviation (*RMSD*) of native and heated proteins in water.

621

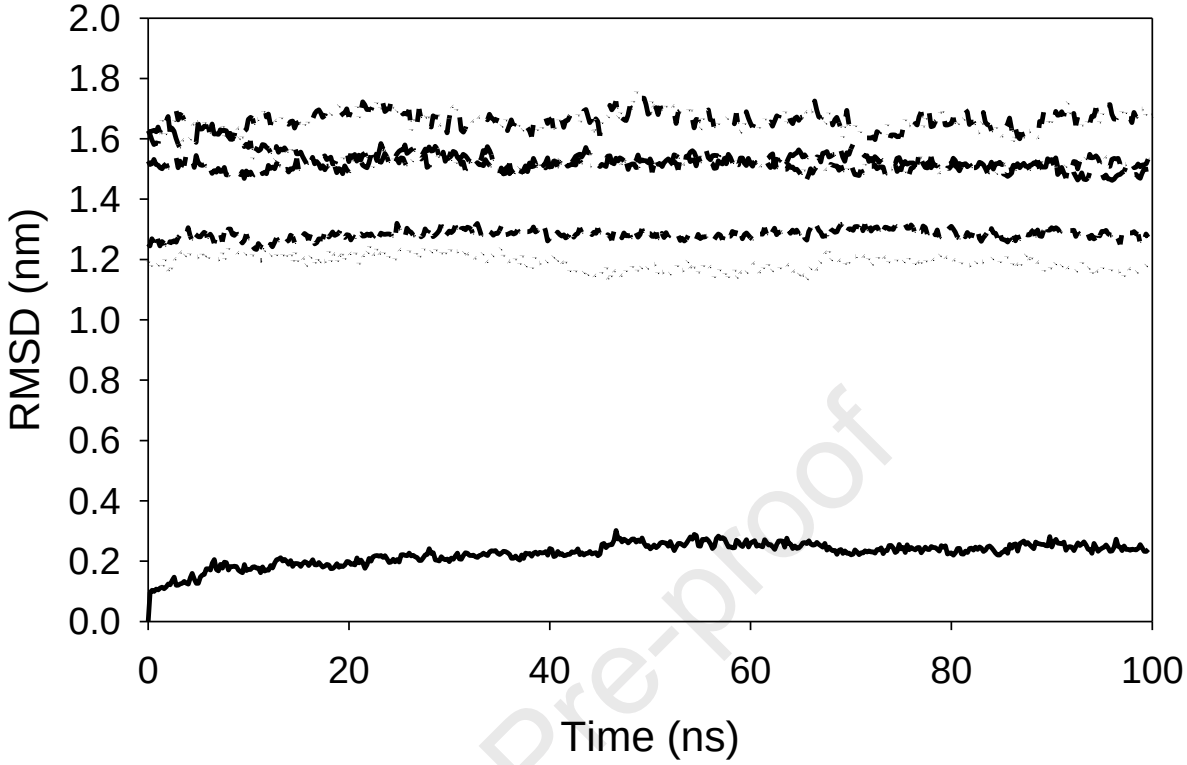

622

623 **Figure 2.** Root mean square deviation (*RMSD*) of native (QO) and different quenched

624 (QI ~ QV) molecules.

625

626

627

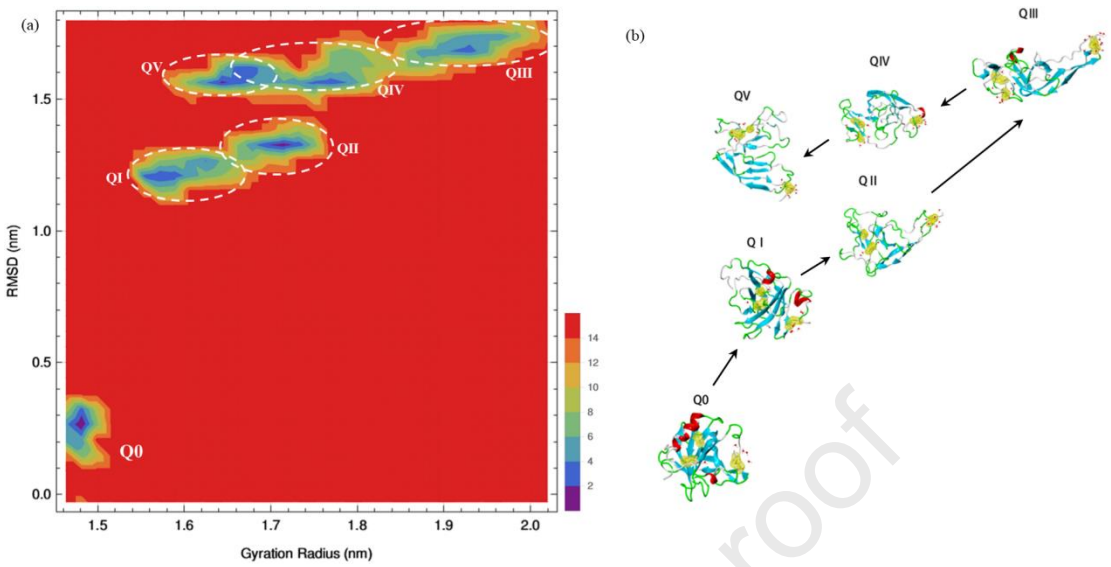

628

629 **Figure 3.** (a) Free Energy Landscapes (FEL): Contour plots of Gibbs free energy versus
630 gyration radius and RMSD from protein structure for different molecules; (b)
631 representative structures of the annealed molecules obtained from FELs (the –SH and
632 S-S residues are labelled by yellow wires and the water molecules around those residues
633 are represented as CPK models).

634

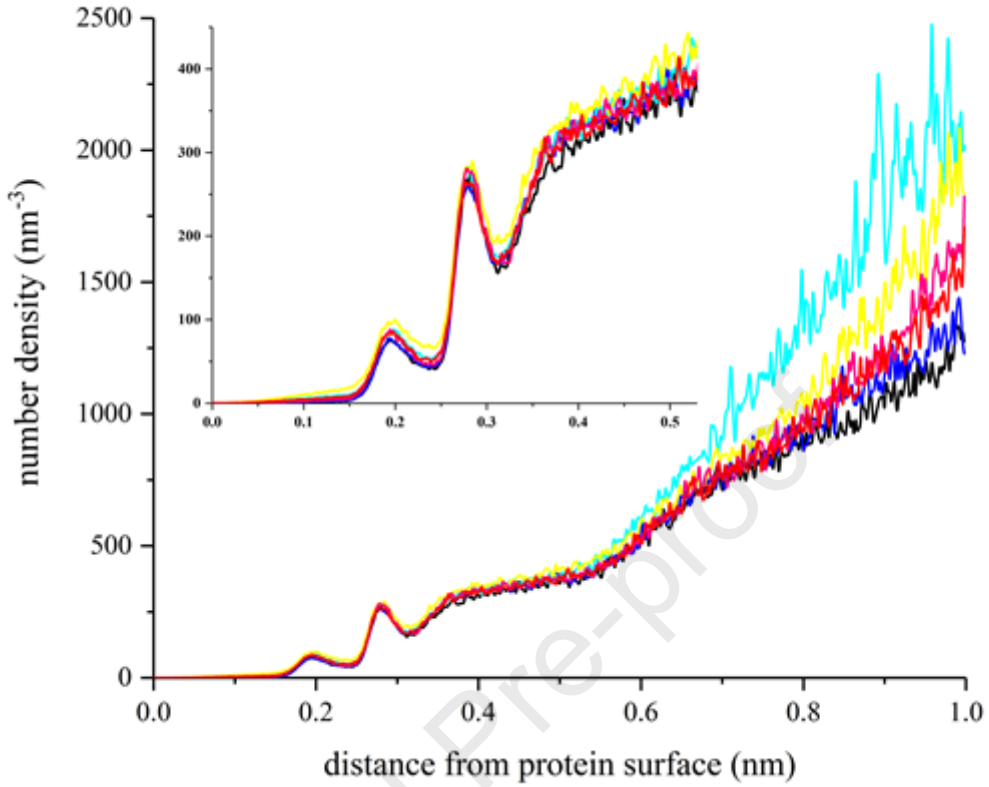

635

636 **Figure 4.** Number density of water molecules (ρ_d[H_2O], counted in terms of the O atom

637 of water) from the surface of the β-lac with the individual conformations, i.e., QO (■),

638 QI (■), QII (■), QIII (■), QIV (■) and QV (■).

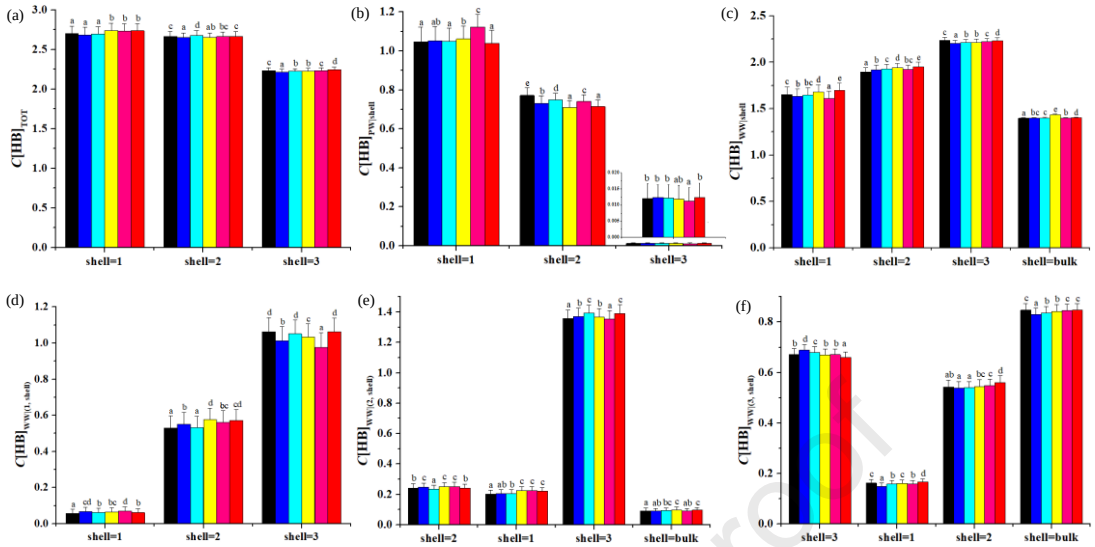

Figure 5. The hydrogen bond (HB) forming capacities of hydration water molecules of β-lac: (a) total HB forming capacities; (b) HB forming capacities with β-lac; (c) HB forming capacities with hydration water molecules themselves; (d) HB forming capacities of hydration water molecules in shell 1 with hydration water molecules; (e) HB forming capacities of hydration water molecules in shell 2 with hydration and bulk water molecules; (f) HB forming capacities of hydration water molecules in shell 3 with hydration and bulk water molecules. Individual β-lac conformations were represented as colour, i.e., QO (■), QI (■), QII (■), QIII (■), QIV (■) and QV (■). Letters 'a, b, c, …' indicate statistically significant differences.

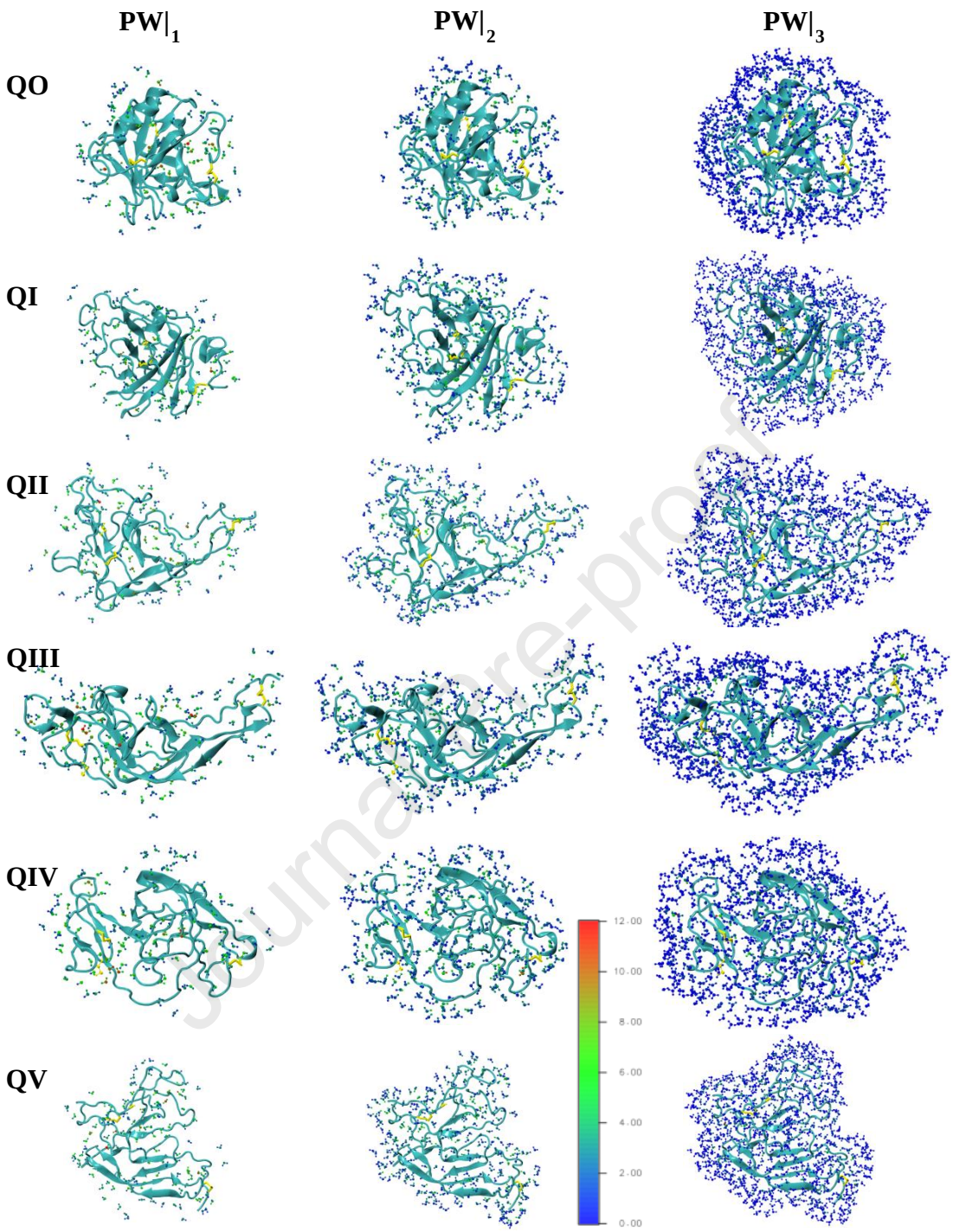

651

652 **Figure 6.** Quantitative interactions between hydration water molecules and the β-lac as

653 evaluated by $10\times\delta g_{inter}$. Red, green and blue atoms indicate strong, intermediate and

654 weak interactions of those water atoms with β-lac.

655

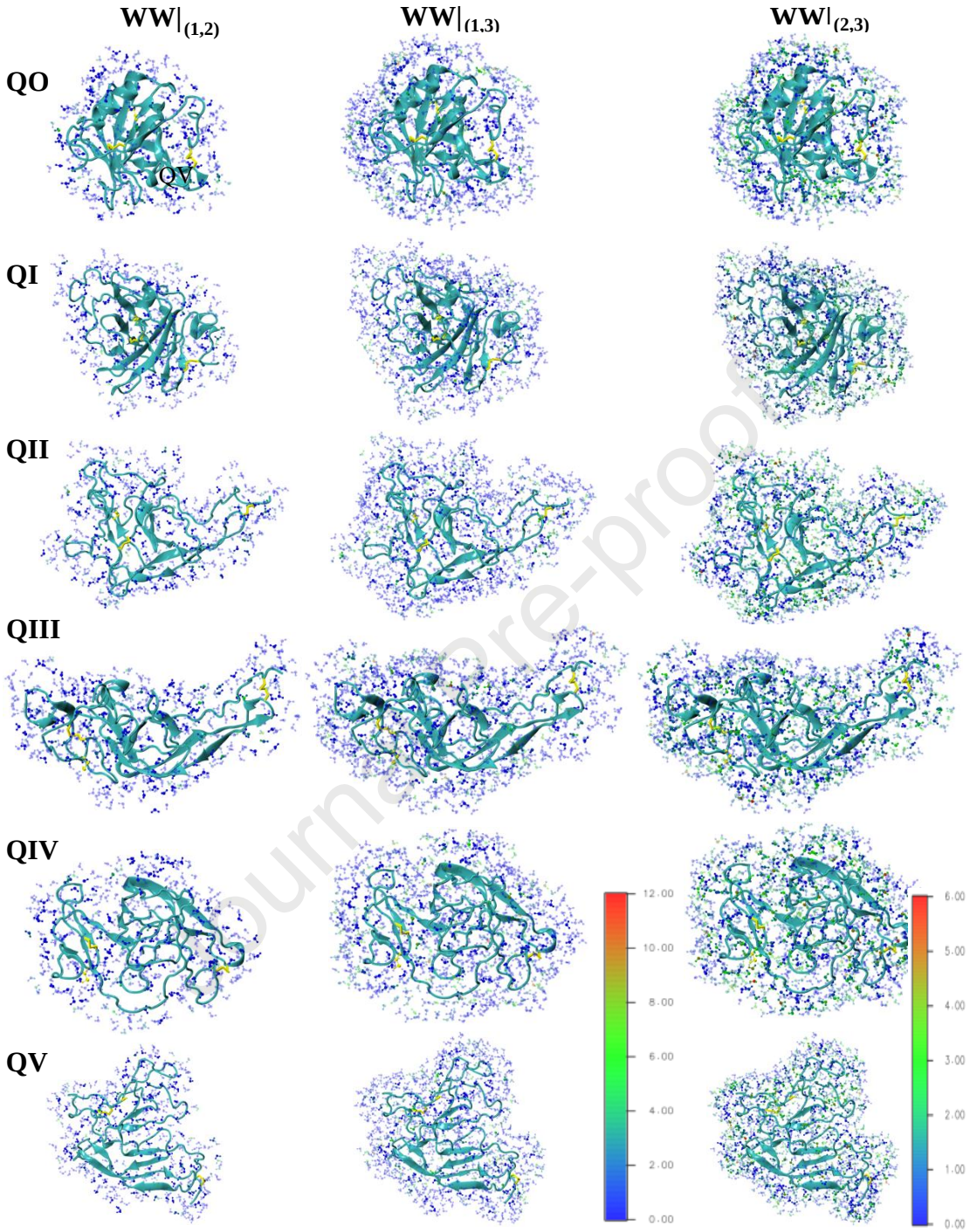

Figure 7. Quantitative interactions between hydration water molecules as evaluated by $10\times\delta g_{inter}$. Red, green and blue atoms indicate strong, intermediate and weak interactions of those hydration water atoms with hydration water atoms in another

661 hydration shell. Transparent water molecules indicate that they are located at a higher

662 hydration shell.

Highlights

- β-lactoglobulin unfolds upon heating through a series of intermediate conformations
- Denatured β-lactoglobulin molecule partially refolded with long-term heating.
- Denaturation changes the structure of the hydration shell around β-lactoglobulin
- Denaturation changes the mobility of water in the hydration shell around β-lactoglobulin
- Unfolding of the β-lactoglobulin increased interactions between hydration shells and the protein and between hydration water molecules themselves.

Conflicts of Interest

The authors declare no conflicts of interest.